

Morphological, biochemical, and phylogenetic assessments of eight *Botryococcus terribilis* strains collected from freshwaters of Transylvania

Adriana Hegedűs · Aurel Mocan ·
Lucian Barbu-Tudoran · Cristian Coman ·
Bogdan Drugă · Cosmin Sicora · Nicolaie Drago

Received: 1 April 2014 / Revised and accepted: 24 July 2014 / Published online: 19 August 2014
© Springer Science+Business Media Dordrecht 2014

Abstract *Botryococcus braunii* is a green unicellular microalga with a unique potential to produce large quantities of hydrocarbons similar to fossil fuel. Up to now, *B. braunii* is the most studied species of the *Botryococcus* genus. The taxonomic affiliation of eight different strains of the genus *Botryococcus* collected from freshwaters of Transylvania was investigated based on their morphological characteristics and molecular profile using small subunit (SSU) ribosomal RNA (rRNA) genes and internal transcribed spacer 2 (ITS2) sequence-structure analysis. The phylogenetic inference using ITS2 sequence-structure molecular marker, an approach addressed for the first time in the issue of *Botryococcus* genus phylogeny, generated similar results with the 18S rRNA gene based analysis. In both phylogenetic trees we constructed, the sequences of our strains formed an independent cluster within the B-race clade. Based on the phylogenetic data and the presence of long mucilaginous processes which emerged from the periphery of the colonies, we established the affiliation of

our strains to *Botryococcus terribilis* species. Detailed analyses regarding the growth performances, ultrastructural characteristics, and hydrocarbon and fatty acid profiles were also included in our study. The micrographs obtained in scanning electron, transmission electron, and light microscopies showed a high degree of similarity to other strains affiliated to the B chemical race. Also, gas chromatography–mass spectrometry assay showed for the first time the ability of *B. terribilis* strains to synthesize C₃₀–C₃₂ botryococcenes, which are known to be specific to the B-type *Botryococcus* strains.

Keywords *Botryococcus terribilis* · Botryococcenes · 18S rDNA · ITS2

Introduction

The genus *Botryococcus* includes green colonial microalgae which are widespread from temperate to tropical freshwater bodies. The feasibility of biofuel production using *Botryococcus* strains (Moldovan and Seifert 1980; Audino et al. 2002; Summons et al. 2002; Ghasemi et al. 2012) is based on their unique potential to synthesize large quantities of hydrocarbons (Largeau et al. 1980a, b; Wake and Hillen 1980, 1981; Hillen et al. 1982; Metzger et al. 1985a). The ability of *Botryococcus* genus to produce different types of hydrocarbons was intensively studied, and four chemical races were defined: (i) the A race, fatty-acid-derived *n*-alkadiene and triene hydrocarbons (Largeau et al. 1980a; Casadevall et al. 1984, 1985; Metzger et al. 1985a, b, 1986, 1993; Metzger and Largeau 2005); (ii) the B race, triterpenoid (squalenes and botryococcenes) hydrocarbons (Ben-Amotz et al. 1985; Wolf et al. 1985; Metzger et al. 1987; Okada et al. 1995; Dayananda et al. 2006); (iii) the L strains, a single

Electronic supplementary material The online version of this article (doi:10.1007/s10811-014-0387-2) contains supplementary material, which is available to authorized users.

A. Hegedűs (✉) · C. Coman · B. Drugă
Institute of Biological Research, 48 Republicii Street,
400015 Cluj-Napoca, Romania
e-mail: adriana.bica@icbcluj.ro

A. Mocan
Institute of Public Health “Professor Iuliu Moldovan”, 6 Pasteur
Street, 400349 Cluj-Napoca, Romania

L. Barbu-Tudoran · N. Drago
Faculty of Biology and Geology, Babeş-Bolyai University, 5-7
Clinicilor Street, 400006 Cluj-Napoca, Romania

C. Sicora
Biological Research Center, 16 Parcului Street, 455200 Jibou,
Romania

tetraterpenoid hydrocarbon named lycopadiene (Metzger and Casadevall 1987); and more recently (iv) the S race, epoxy-*n*-alkane and saturated *n*-alkane chains with 18 and 20 carbon atoms (Kawachi et al. 2012). Except for the chemical classification, the taxonomy of the genus *Botryococcus* is still unclear. Although most of the studies assigned the investigated strains to *Botryococcus braunii* species (Watanabe and Tanabe 2013), some authors emphasized the morphological heterogeneity (Komárek and Marvan 1992) and the phylogenetic divergence of *Botryococcus* genus (Kawachi et al. 2012). The last group of authors established the relationship between the above mentioned four chemical races and their phylogenetic profile based on 31 new *Botryococcus* isolates.

Using 47 *Botryococcus* populations collected from different biotopes all over the world, Komárek and Marvan (1992) described 13 morphotypes (including the known species *B. braunii* (Kützing 1849) *Botryococcus protuberans* (Komárková 1991), and *Botryococcus canadensis* (Hindák 1991)), and they defined six new species: *Botryococcus comperiei*, *Botryococcus australis*, *Botryococcus fernandoi*, *Botryococcus neglectus*, *Botryococcus pila*, and *Botryococcus terribilis*. Plain et al. (1993) contested the morphological features as reliable criteria to distinguish among *Botryococcus* species due to the inherent morphological changes within a clonal strain. Thus, the plasticity of morphological characters remains a crucial aspect in solving the taxonomic issue of the genus.

According to Komárek and Marvan (1992), the distinctive morphological feature of *B. terribilis* colonies is the presence of “short or long, simple or irregularly branched gelatinous processes” emerging from the periphery of the colonies. This species was signaled in Cuba (Komárek and Marvan 1992; Comas 1996), Brazil (Nogueira and Oliveira 2009; Rodrigues et al. 2010; de Queiroz Mendes et al. 2012; Nascimento et al. 2013), Spain (Fanés Treviño et al. 2009), Sweden, Austria, Chad, and Czech Republic (Komárek and Marvan 1992). In a recent study, de Queiroz Mendes et al. (2012) outlined the morphological and ultrastructural characters of a newly isolated strain of *B. terribilis* (FW-15) which agree in general aspects with the original description of Komárek and Marvan (1992) and with other strains belonging to *B. braunii* species (Wolf and Cox 1981; Berkaloff et al. 1984; Largeau et al. 1980b; Casadevall et al. 1985; Metzger and Largeau 2005; Weiss et al. 2012).

In the present study, we aimed to establish the taxonomic affiliation of eight *Botryococcus* strains isolated from Transylvania (Romania), based on morphological characters supported by molecular data. To increase the resolution of the phylogenetic analysis, both the small subunit ribosomal RNA (rRNA) gene sequences and the internal transcribed spacer 2 (ITS2) sequence structures were used in the study. The ultrastructural and biochemical characteristics of the investigated strains were also included in our analysis.

Materials and methods

Strain cultures and growth assay

Eight *Botryococcus* strains were investigated in this study (see the list in Online Resource 1): AICB 413, AICB 414, AICB 416, AICB 418, AICB 440, AICB 442, AICB 870, and AICB 872. *Botryococcus* isolates are deposited in the Algae and Cyanobacteria Culture Collection of the Institute of Biological Research (AICB), Cluj-Napoca, Romania (Drago et al. 1997). The strains were grown on BG-11 medium (Allen and Stanier 1968; Watanabe et al. 2000), in continuous irradiance of approximately 150 $\mu\text{mol photons m}^{-2} \text{s}^{-1}$, 25 ± 2 °C, in aerated flasks (500 mL). Optical density (OD) measurements at 600 nm were taken every 2 days. In late exponential growth phase (approximately 30 days), the biomass was harvested and aliquoted for subsequent morphological, biochemical, and molecular analyses. Aliquots of 50 mL were filtered and washed two times with distilled water to assess the dry weight. The samples were dried (70 °C) to constant weight (at least 24 h). The growth process was characterized by the doubling time and the chlorophylls to carotenoids ratio relative to the dry weight. The doubling time was calculated following the formula of Guillard (1973). The assimilatory pigments were quantified based on Arnon (1949), Goodwin (1976), and Britton et al. (1995) protocols.

Light and electron microscopy

Light microscopy was performed using an Olympus BX-41 microscope equipped with a photo camera. For scanning electron microscopy (SEM), algal samples were concentrated by centrifugation and washed two times with 0.1 M sodium phosphate buffer (pH 6.8), followed by a final wash with distilled water. The cells were fixed in 4 % glutaraldehyde in sodium phosphate buffer (4 °C) overnight and then fixed on copper holders, covered by a 7-nm silver or gold layer. The images were taken with a Jeol JSM5510ILV electron microscope. For transmission electron microscopy (TEM), fresh colonies were collected by centrifugation, fixed in 4 % glutaraldehyde for 1 h, and rinsed four times with 0.1 M sodium phosphate buffer (pH 6.8). Subsequently, the biomass was resuspended in 2 % OsO₄ in phosphate buffer, for 1 h. The fixed material was dehydrated through a graded ethanol series and treatment with propylene oxide. The samples were embedded in a mix of propylene oxide and Epon 812 resin. A TEM Jeol JEM1010 microscope was used to observe the thin sections.

Hydrocarbon (HC) and fatty acid (FA) analyses—gas chromatography–mass spectrometry (GC-MS)

Chloroform, methanol, and water extraction mix 1:1:0.5 (v/v/v) was used to extract HC and FA from wet biomass (Bligh and Dyer 1959; Sutherland and Wilkinson 1971). Each chloroform sample was used to establish both HC and FA contents. Methanol and acetyl chloride were used to convert FA to methyl esters (FAMES) (Christie 1993). An aqueous solution of sodium chloride (36 %) was added to FAME samples, subsequently followed by extraction in *n*-hexane. The HC chloroform extracts were concentrated and dissolved in *n*-hexane also. Both types of *n*-hexane samples were inspected using an Agilent Technologies 6890 N gas chromatograph coupled with an Agilent Technologies 5973 N mass spectrometer. The samples were analyzed on HP-1 (0.25 mm×30 m) and HP-5 (0.32 mm×50 m) columns, using a flame ionization detector (FID). Chromatographic conditions were as follows: nitrogen as carrier gas for FID and helium for the mass spectrometer; flow rate 1–2 mL min⁻¹; sample input temperature 280 °C, rate of temperature increase to 280 °C, 10 °C min⁻¹; and transfer line temperature 280 °C. HC and FA were identified by mass spectra of the samples, at 70 eV, based on their retention time. The HC values were converted into percentages relative to dry weight. Relative content of FA was calculated based on the normalization method. By this method, the areas of all peaks in the chromatograms were summed, and the content of each fatty acid was expressed as percentage of the summed areas (Poole 2003).

DNA extraction, PCR amplification, and DNA sequencing

Wizard SV Genomic DNA Purification System (Promega, USA) was used to isolate genomic DNA, according to the manufacturer's instructions. The polymerase chain reaction (PCR) and DNA sequencing of small subunit (SSU) rRNA genes were carried out with the primers used by Sawayama et al. (1995) and Senousy et al. (2004). In addition, we designed a pair of primers (CV5 and 28S CD1RBbB) to amplify and sequence the ITS1-5.8S-ITS2 DNA region: 5'-CCGATTGGGTGTGCTGGTGAAGC-3' (forward) and 5'-TTCA GCGGGTGCTCTTACCT-3' (reverse). Fast PCR 6.4 software (Kalendar et al. 2011) was used to design and test the primers. The PCR mix contained 1.25 units of DreamTaq DNA Polymerase (Fermentas, Canada) in the manufacturer's buffer, 1.5 mM MgCl₂, 0.2 mM dNTP, and 0.4 μM primer in a final volume of 50 μL. The tubes were incubated using a TGradient thermal cycler (Biometra, Germany) with an initial denaturation at 95 °C for 5 min followed by 32 cycles of 95 °C for 45 s, 56 °C for 55 s, 72 °C for 2 min, and a final incubation at 72 °C for 10 min. Electrophoresis

was performed in 1 %w/v agarose gel (stained with 1 μg mL⁻¹ ethidium bromide), and photographs were taken with the BioDoc-it Imaging System (UPV, Analytik Jena AG, Germany). Direct sequencing was carried out subsequent to PCR product purification (Wizard SV Gel and the PCR Clean-Up System, Promega, USA) following the manufacturer's instructions. The samples were processed with the ABI Prism BigDye Sequencing Kit (Applied Biosystems, USA) and transferred in an ABI Prism 3130 genetic analyzer, according to the protocol. The sequences were submitted to GenBank (Benson et al. 2008), accession numbers JF261251, JF261252, JF261254, JF261256, JF261258, and KJ541889-KJ541891.

Phylogenetic analysis of 18S rDNA and ITS2 fragments

Sixty SSU ribosomal DNA (rDNA) sequences from GenBank, belonging to the genera *Botryococcus*, *Chlorella*, *Choricystis*, *Neochloris*, and *Dictyosphaerium* were used in the analysis. The homologous sequence of *Ulva compressa* C184 was used as outgroup. The multiple alignments and construction of the phylogenetic trees were carried out with MEGA 6.06 (Tamura et al. 2013). Maximum likelihood (ML), maximum parsimony (MP), and neighbor-joining (NJ) algorithms were used to infer phylogeny. Bootstrap values for the trees were calculated from 1,000 replicates (NJ and MP) and 100 replicates (ML) respectively. TrN+G (Tamura and Nei 1993) (variable base frequencies, equal transversion rates, variable transition rates with the gamma distribution) was the best fit evolutionary model for ML, based on JModelTest 0.1.1 results validated with both Akaike information criterion (AIC) and Bayesian information criterion (BIC) (Guidon and Gascuel 2003; Posada 2003). Twenty ITS2 sequences including their secondary structure were retrieved from the ITS2 Database (<http://its2.bioapps.biozentrum.uni-wuerzburg.de/>) (we included here all the *Botryococcus* ITS2 sequences present at the time in this database) (Schultz et al. 2006; Selig et al. 2008; Koetschan et al. 2010, 2012). They were affiliated to *B. braunii* species (13 sequences) and to other genera of the phylum Chlorophyta (seven sequences). The homologous sequence of *Ulva rigida* UrigVM was chosen as outgroup. The multiple sequence-structure alignment was calculated with 4SALE (Seibel et al. 2006, 2008). A profile neighbor-joining (PNJ) tree was calculated by ProfDistS (Müller et al. 2004; Friedrich et al. 2005; Rahmann et al. 2006; Wolf et al. 2008) using general time reversible (GTR) substitution model (Lanave et al. 1984). The tree was edited with TreeView (Page 1996). A second multiple sequence alignment was performed with MEGA 6.06 using the same ITS2 sequences. The GTR substitution model was used to construct the ML tree based on 100 replicates.

Results

Morphology and ultrastructure

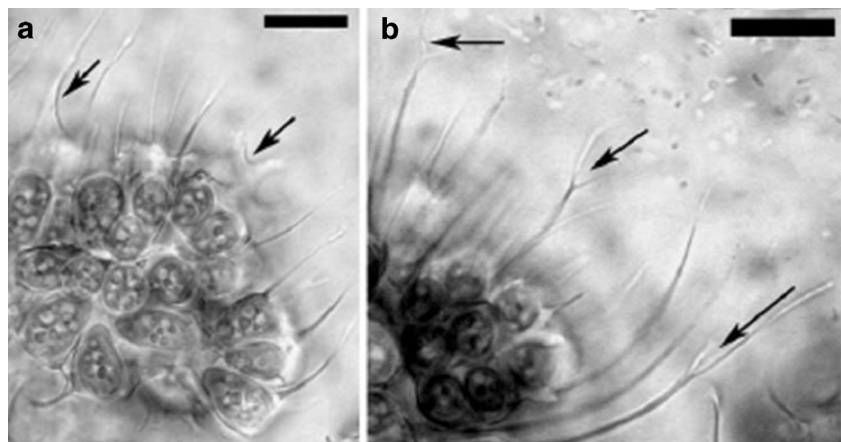
The morphological features of the AICB strains agreed in general aspects with the descriptions of other *B. terribilis* strains (Komárek and Marvan 1992; Fanés Treviño et al. 2010; de Queiroz Mendes et al. 2012). Thus, the colonies of AICB strains exhibited typical features which resemble the botryoid organization characterized by pyriform-shaped cells (Fig. 1), embedded in a hydrocarbon-rich matrix (Fig. 2). Irregularly, large colonies, from 35 to 454 μm (but the majority not exceeding 100 μm), appeared rather tight and held together by refringent hydrocarbon string-like connections (Fig. 2d, f, g, h). A fibrillar sheath spans into the growth medium and surrounds the entire algal colony (Fig. 3a). Long and sometimes branched mucilaginous processes (Fig. 1) which are known to be specific to the species *B. terribilis* (Komárek and Marvan 1992) were seen at the periphery of the colonies. The structures (when present) that linked the subcolonies showed different patterns: (i) long, fine, thread-like structures (Fig. 2e); (ii) shorter and sheet-like strands (Fig. 2h); (iii) very short and numerous formations (Fig. 2f, g); and (iv) irregularly shaped, rather thick connections (Fig. 2d). Each cell was protected by a cup-shaped envelope which covered almost its entire surface. In most of the investigated strains, the cells were completely hidden within the hydrocarbon matrix or slightly emerged from it (Fig. 2b, c), as in the case of other *B. terribilis* strains described by Komárek and Marvan (1992), Fanés Treviño et al. (2010), and de Queiroz Mendes et al. (2012).

The electron micrographs of the matrix revealed the presence of superimposed cell walls (trilaminar structure, TLS) immersed in liquid hydrocarbons (Figs. 2c and 3b, c, e). As previously observed (Wolf and Cox 1981; Berkloff et al. 1984), the sandwich aspect of the cell walls was characterized by a visible electron lucent material, associated with electron dense fragments on one or both sides. Concentric TLSs which

alternated with liquid hydrocarbons were present around both solitary and dividing cells (Fig. 3b). An electron dense thick cell wall (CW) was observed in direct contact with the plasma membrane. Its outer side was covered by a thin layer (T) of the above mentioned electron-lucent material (Fig. 3e, g, h). In addition, at the cell apex, the T layer was coated by an electron dense layer (G) ended by well-developed anastomosing fibrils (F) which spanned into the growth medium (Fig. 3e, f). The aspect of the G and F layers was very much alike the description of the granular and the fibrillar layers of the retaining wall (RW) made by Weiss et al. (2012) in the case of *Showa* (Berkeley) strain (hereafter, we will use the same terminology). Figure 3e, f, and h show that the RW extended along the external face of the matrix and occasionally falls within creating hydrocarbon folds. When cells are adjacent, the RW formed zipper-like structures as described by Weiss et al. (2012) (Fig. 3d). Round to oval liquid hydrocarbon droplets were seen outside the plasma membrane and the associated CW–T structure, contributing to the lateral extension of the matrix. Interestingly, in some micrographs, liquid hydrocarbon drops occurred between two successive cell walls (Fig. 3g, h). Lipid droplets were never present in the apical region of the cells which occasionally displayed an electron dense material, the so-called “cap” (Wolf and Cox 1981). When present, the cap was always located between two consecutive CW–T layers. The outer CW–RW association projected its fibrils outside the colony (Fig. 3f, g, h). The occurrence of the cap was observed, especially in the cells where lipid droplets accumulated in the lateral parts, filling the space between the two adjacent CW–T cell walls (Fig. 3g, h).

The pyriform cells, 5 to 12 μm in length, usually not exceeding 9 μm , are more or less radially oriented with length-to-width ratio of up to 2:1. The cup-shaped chloroplast was placed adjacent to the plasma membrane (Fig. 3e, g). Occasionally, starch granules were observed within the chloroplast (Fig. 3c). The pyrenoid penetrated by chloroplast lamellae was located at the bottom of the cell (Fig. 3b, g). The nucleus was centrally located (Fig. 3d, g). Strands of

Fig. 1 Light microscopy of *B. terribilis* AICB 413 and 440 strains. **a** The pyriform-shaped cells are disposed radially. The colonies of AICB 413 strain presented mucilaginous processes at the periphery which are rather thick at their base (indicated by arrows); **b** AICB 440. Long, fine, and sometimes branched (indicated by arrows) mucilaginous processes are shown in the AICB 440 strain. Bar=10 μm



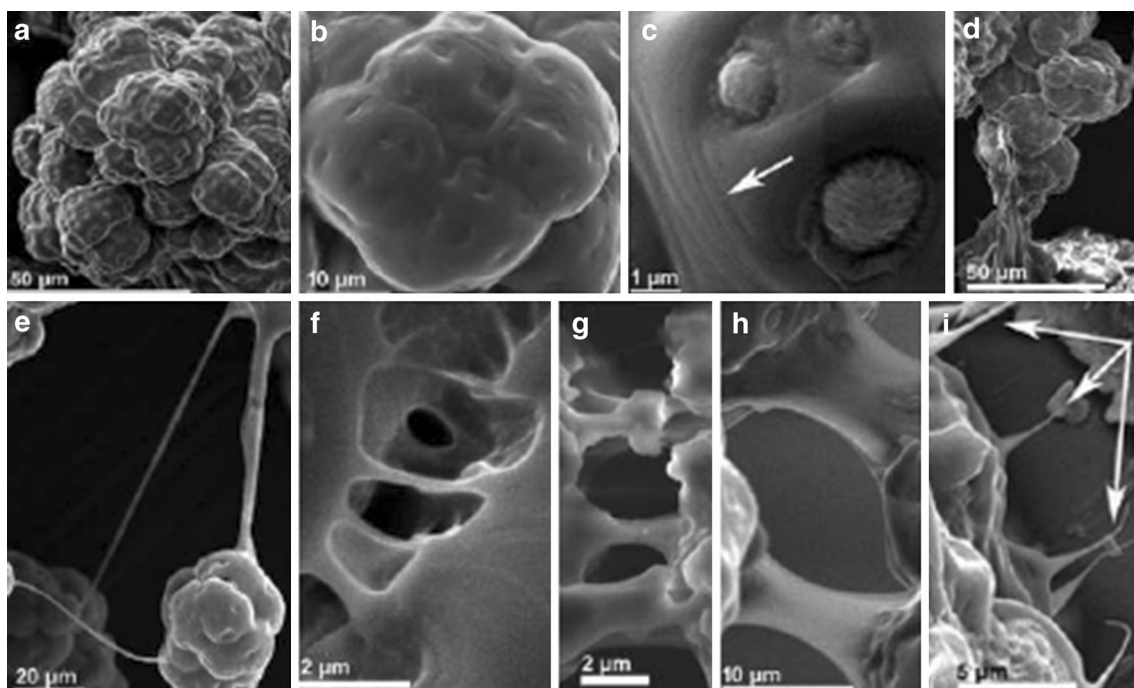


Fig. 2 Scanning electron microscopy of *B. terribilis* AICB strains. The colonies contain tight subcolonies (**a** AICB 413) with cells completely (**b** AICB 442) or partially embedded (**c** AICB 416) in the hydrocarbon matrix, which consists of a succession of hydrocarbon folds indicated

by a white arrow (**c**). Different patterns of hydrocarbon connections between subcolonies are shown (**d** AICB 440, **e** AICB 442, **f** AICB 416, **g** AICB 872, **h** AICB 413). Long mucilaginous processes emerge from the periphery of the colonies (indicated by arrows in **i** AICB 442)

endoplasmic reticulum (ER) were seen adjacent to the chloroplast, plasma membrane, and sometimes surrounding the lipid bodies (LB) (Fig. 3c). More or less large lipid bodies were observed within the cavity of the chloroplast body (Fig. 3c, g). Golgi body was observed in close vicinity with the cell apex (Fig. 3e). The cell-harbored mitochondria, vacuoles, and sometimes polyphosphate bodies (PB) were observed (Fig. 3c, e, g).

Growth assay

The growth parameters are summarized in Table 1. According to our experiments, AICB 413, 414, 416, 418, 442, 870, and 872 grew the most rapidly, while the rate of divisions was lower in the case of the AICB 440 strain. The AICB 870 culture showed the lowest doubling time (2.10 days), whereas the highest value was obtained for the AICB 440 strain which doubled every 4.6 days (Table 1). According to the Chl/Car ratio, in six of the eight inspected AICB strains, the value varied from 1.33 (AICB 440) to 2.37 (AICB 416). A distinctive pattern was noted though in the case of AICB 870 and 872 strains which showed higher values of this ratio (3:1), due to the larger quantities of chlorophylls (data not shown).

Hydrocarbons

For each AICB strain, GC-MS analysis of hydrocarbons was performed on two chloroform extracts, derived from different

cultures. The AICB strains synthesized four types of hydrocarbons: C_{29} alkadienes (2Δ) and C_{30} – C_{32} triterpenes (6Δ), known as botryococcenes, although the C_{30} botryococcene was not identified in the biomass of the AICB 416 and 870 strains (Table 2). The chromatograms revealed different amounts of hydrocarbons ranging from 8.46 % (AICB 870) to 25.74 % (AICB 413) of dry weight (Table 2). In all chloroform extracts, C_{31} and C_{32} botryococcenes presented as major fractions (Table 2). These compounds accounted for at least 70 % of the hydrocarbons synthesized by the AICB strains (Table 3).

Fatty acids

Twelve types of fatty acids classified as saturated (SFA) and unsaturated (UFA) were identified in the chloroform extracts resulting from processing the biomass of the AICB strains (Table 4). The percentage of UFA (75.10 %) exceeded approximately three times the percentage of SFA (24.88 %) (Table 4). This ratio characterized the fatty acid profile of each strain with the exception of AICB 418 (two times higher) and AICB 442 (four times higher) (Table 4). Some fatty acids were not identified in the extracts of four investigated strains. These are arachidic acid (in AICB 414, 418, and 872), arachidonic acid (in AICB 870), lauric acid (in AICB 870 and 872), and docosahexaenoic acid (DHA) (in AICB 870) (Table 4). In addition, the first three fatty acids were scarcely present in the rest of the AICB strains investigated. Myristic,

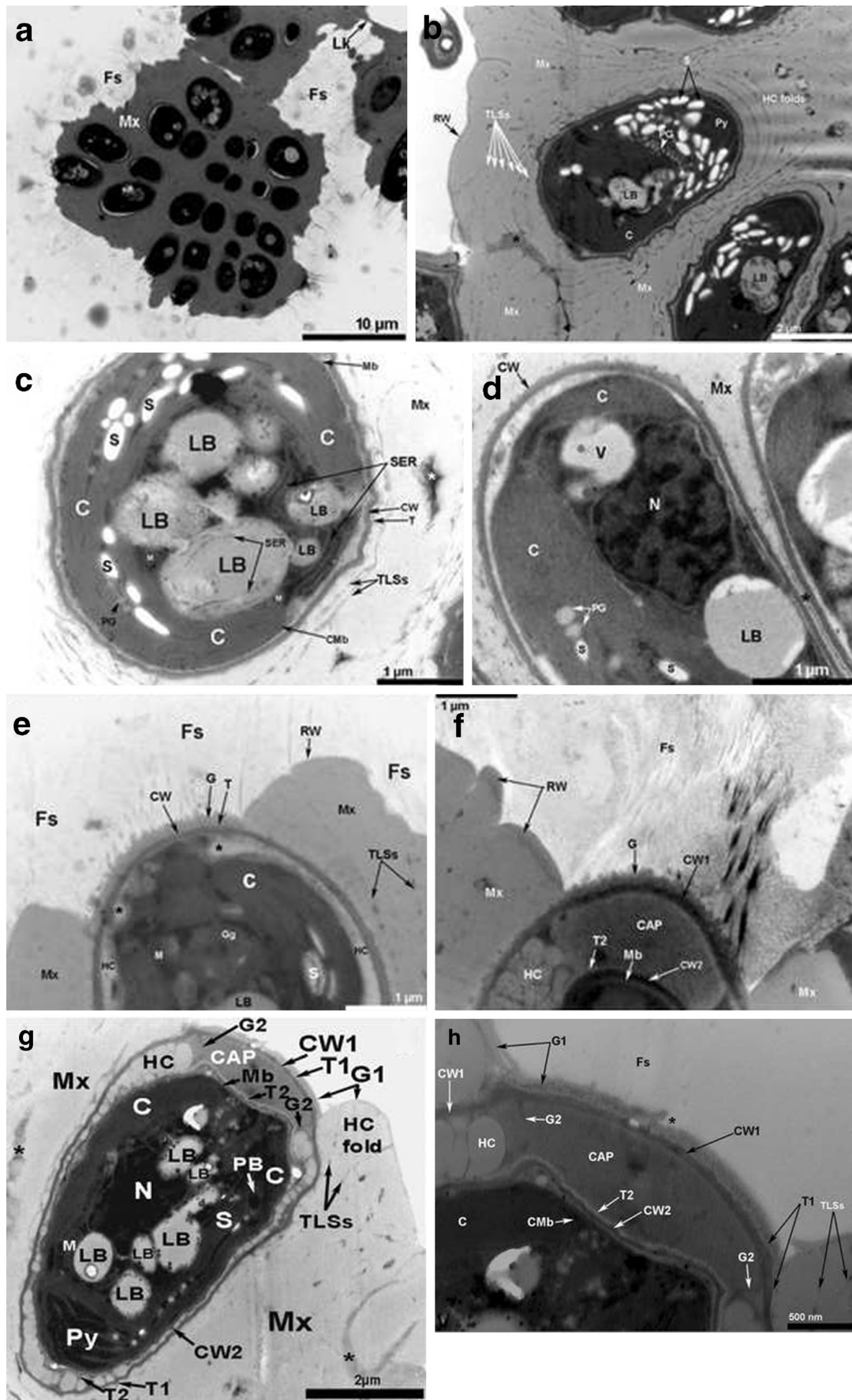


Fig. 3 Ultrastructure of *B. terribilis* AICB 416 (a, e, f) and 442 (b, c, d, g, h) strains. *Fs* fibrils, *Lk* mucilaginous connections, *RW* retaining wall, *TLSs* trilaminar structures, *HC* hydrocarbons, *Py* pyrenoid, *C* chloroplast, *PG* plastoglobules, *LB* lipid bodies, *S* starch, *M* mitochondria, *SER* smooth endoplasmic reticulum, *CW* cell wall, *CW1* old cell wall, *CW2* new cell wall, *T* tubular layer, *T1* old tubular layer, *T2* new tubular layer, *CMb* chloroplast envelope, *Mb* cell membrane, *V* vacuole, *N* nucleus, *G* granular layer, *G1* old granular layer, *G2* new granular layer, *Gg* Golgi body, *PB* polyphosphate body, *CAP* apical cap. **a** The fibrillar sheet surrounding the colony and the mucilaginous connections are shown. **b** The HC matrix which consists of successions of TLS and HC folds is displayed. **c** The presence of LB, SER, and C filled with S granules was observed. **d** The presence of a zipper-like structure (pointed out by *asterisk*) between adjacent cells is shown. **e** Details regarding the presumptive formations of the cap in the apical part of cell (pointed out by *asterisks*). **f** Details of fibrillar layer and the aspect of the apical cap (CAP) are shown. Ultrastructure of *B. terribilis* AICB 442 strain. **g** Details regarding the apical cap (CAP), cell wall, and ultrastructural aspects are shown. Putative remains of the old granular layer are shown by *asterisk*. **h** Details of apical cap and cell walls. A possible place of old cell wall rupture is pointed out by *asterisk*

palmitoleic, and stearic fatty acids were also identified as small fractions in all the AICB strains (Table 4). Overall, the C₁₆ (palmitic) and C₁₈ (oleic, linoleic, and linolenic) fatty acids were found as major fractions in the fatty acid extracts from all the AICB strains (Table 4). Our GC-MS results outlined the presence of oleic acid (27.38 %) as the most abundant fraction among fatty acids followed by linolenic (16.69 %) and palmitic acids (16.15 %), closely accompanied by linoleic acid (14.40 %). Although the specific order of these major fractions was slightly different among the AICB strains (Table 4), they were present as dominant relative amounts in all AICB extracts.

Interestingly, ω-3 DHA and eicosapentaenoic acid (EPA) were both present in significant relative amounts in all the studied strains, except for the AICB 872 strain which contained only EPA (20.18 %). The ω-3 fatty acids reached values of up to 20 % of the total fatty acids, with highest values in the AICB 872 and AICB 870 strains (Table 4).

Table 1 The doubling time and the chlorophyll-to-carotenoid ratio of *B. terribilis* AICB strains

AICB strain	Doubling time (days)	Chl/Car ratio % of dry weight (w/w)
413	2.77	2.06
414	3.15	1.47
416	2.91	2.37
418	3.47	1.99
440	4.62	1.33
442	2.77	1.83
870	2.10	2.98
872	2.39	3.41

Table 2 Total hydrocarbon level (as percent of dry weight) produced by the *B. terribilis* AICB strains

Strain code	Botryococcenes (6Δ)			Alkadienes		
	6ΔC ₃₀	6ΔC ₃₁	6ΔC ₃₂	Total (6Δ)	(2Δ) 2ΔC ₂₉	Total HC
413	0.39	10.13	10.19	20.71	5.03	25.74
414	0.02	0.67	10.65	11.34	2.66	14.00
416	0.00	8.26	5.76	14.02	4.93	18.95
418	1.96	6.94	7.60	16.50	0.87	17.37
440	0.23	15.46	8.40	24.09	1.02	25.11
442	0.35	11.41	6.58	18.34	2.84	21.18
870	0.00	0.32	7.26	7.58	0.88	8.46
872	0.32	1.56	15.85	17.73	0.85	18.58

Phylogenetic placement of AICB strains based on SSU rDNA and ITS2 sequences

In addition to the molecular approaches which used the 18S rRNA genes (Plain et al. 1993; Sawayama et al. 1995; Senousy et al. 2004; Weiss et al. 2010, 2011; Kawachi et al. 2012), we selected the ITS2 sequence as a second marker in the phylogenetic analysis of the AICB strains. The ITS2 fragments have been used in other studies which aimed to solve phylogeny issues at the genus or species level (Olsson et al. 2009; Merget and Wolf 2010). Even though the ITS2 sequence is poorly conserved, its secondary structure presents a high degree of conservation (Schultz et al. 2005). Thus, we decided to use both the sequence and the secondary structure in our approach. As shown in Figs. 4 and 5, all the *B. terribilis* AICB sequences grouped within the cluster of strains affiliated to the B chemical race, being closely related to Showa and Bot 24 sequences. Among the *B. terribilis* AICB strains, AICB 870 and 872 formed a distinct cluster, supported by bootstrap values of 64/89/63 (obtained by using NJ, MP, and

Table 3 Relative amounts of hydrocarbons (as percent of total) produced by the *B. terribilis* AICB strains

Strain code	Botryococcenes (6Δ)			Total (6Δ)	Alkadienes (2Δ) 2Δ C ₂₉ 2Δ	Total HC
	6ΔC ₃₀	6ΔC ₃₁	6ΔC ₃₂			
413	1.51	39.36	39.59	80.46	19.54	100
414	0.14	4.79	76.07	81.00	19.00	100
416	0.00	43.58	30.40	73.98	26.02	100
418	11.28	39.95	43.76	94.99	5.01	100
440	0.92	61.57	33.45	95.94	4.06	100
442	1.65	53.87	31.07	86.59	13.41	100
870	0.00	3.78	85.82	89.60	10.40	100
872	1.72	8.40	85.31	95.43	4.57	100

Table 4 Fatty acid composition of *B. terribilis* AICB strains

Fatty acid	AICB 413	AICB 414	AICB 416	AICB 418	AICB 440	AICB 442	AICB 870	AICB 872	Average
Lauric (12:0)	1.03	1.64	1.85	3.66	0.88	0.82	n.d.	n.d.	1.24
Myristic (14:0)	2.67	2.70	3.46	4.97	2.34	1.57	2.09	2.03	2.73
Palmitic (16:0)	16.61	14.03	15.87	22.12	15.36	12.55	18.66	14.02	16.15
Palmitoleic (14:1)	4.15	3.12	2.15	5.63	2.00	1.94	1.27	0.94	2.65
Stearic (18:0)	4.42	4.43	2.49	4.24	3.75	2.28	3.09	4.29	3.62
Oleic (18:1)	23.92	35.97	34.51	16.64	30.81	38.12	15.62	23.49	27.38
Linoleic (18:2)	14.33	17.29	12.17	5.55	9.75	3.78	11.27	25.10	12.40
Linolenic (18:3)	17.06	11.80	13.42	26.19	14.20	16.26	26.56	8.05	16.69
Arachidic (20:0)	1.38	n.d.	2.46	n.d.	1.67	2.37	1.26	n.d.	1.14
Arachidonic (20:4)	4.04	0.25	2.92	1.91	5.10	3.06	n.d.	1.61	2.36
EPA (20:5)	5.23	0.18	3.55	4.44	6.81	8.22	20.18	8.78	7.17
DHA (22:6)	5.17	8.60	6.56	4.67	7.35	9.01	n.d.	11.67	6.63
SFA	26.11	22.79	26.14	34.98	23.98	19.59	25.10	20.34	24.88
UFA	73.87	77.20	73.82	65.01	76.01	80.38	74.90	79.64	75.10

The results are given as percentage of total fatty acids

EPA eicosapentaenoic acid, *DHA* docosahexaenoic acid, *SFA* saturated fatty acids, *UFA* unsaturated fatty acids, *n.d.* undetectable

ML methods) in the 18S rRNA gene analysis (data not shown). This grouping was also observed in the ITS2 analysis, the cluster being supported by a maximal bootstrap value, probably due to the low number of ITS2 sequences. To ease the comparison between the SSU rDNA and the ITS2 analyses, we used all *Botryococcus* sequences containing both the 18S gene and the ITS2 fragment, available at the time in the public databases (GenBank accession numbers AJ581910, AJ581911, GU951519, GU951520, and AJ581912). These sequences were placed in the same clades in both phylogenetic trees (Figs. 4 and 5), giving credit to the ITS2 analysis where the number of available *Botryococcus* ITS2 sequences was low. The phylogenetic inference based on the SSU rDNA and ITS2 sequences revealed the existence of five (18S rDNA) and four (ITS2) distinct groups of taxa (Figs. 4 and 5). Three major clades (supported by significant bootstrap values) were formed by *Botryococcus* sequences which separated according to their chemical race (A, B, and S/L). As stated by previous studies on SSU rDNA fragments (Kawachi et al. 2012), our data pointed out that the B and the S/L clades are more closely related to each other than to the A clade. In addition, the B and L groups possess a common isoprene origin of their terpenic hydrocarbons (Baba and Shiraima 2013). The close phylogenetic relationship between *Botryococcus* and *Choricystis* was certified by the high bootstrap values obtained in the 18S rDNA approach (Fig. 4). Unfortunately, we could not extend this conclusion to the ITS2 analysis, for the reason that no ITS2 sequences belonging to *Choricystis* genus were yet submitted in the ITS2 database. Although a low number of *Botryococcus* ITS2 sequences was used in the analysis, this outcome is sustained by the PNJ/ML tree.

Discussion

Morphology and ultrastructure

Although strains identified as *B. braunii* are currently used in most studies, our results pointed out differences between the aforementioned species and our AICB strains. The transitory occurrence of simple or irregularly branched gelatinous processes (Komárek and Marvan 1992) was obvious in all investigated AICB strains. This feature was used by the above mentioned authors as one of the most important diagnostic characters in identifying *B. terribilis* species. The presence of these processes was also noticed in other strains of *B. terribilis* (Fanés Treviño et al. 2010; de Queiroz Mendes et al. 2012). Considering that similar mucilaginous processes were never observed in the case of *B. braunii*, we followed the description of the *B. terribilis* strains made by Komárek and Marvan (1992) and de Queiroz Mendes et al. (2012). The data obtained by these authors will be briefly reiterated along with additional conclusions. Thus, the algal colonies of the AICB strains were more or less irregularly, brownish or yellowish, extending 100 µm in diameter, dimensions which fitted the Brazilian strain (de Queiroz Mendes et al. 2012), but not the strains analyzed by Komárek and Marvan (1992). The connections between subcolonies of the AICB strains exhibited more varied patterns (Fig. 2d–h) than the short string-like firm gelatinous connections described by both groups of researchers. Similar to the Brazilian strain (FW-15), each AICB strain showed colonies with cells both completely embedded in the matrix and with their apex protruding from the envelope (Fig. 2b, c) (observation also made, with caution, by Komárek and Marvan 1992). This characteristic could be

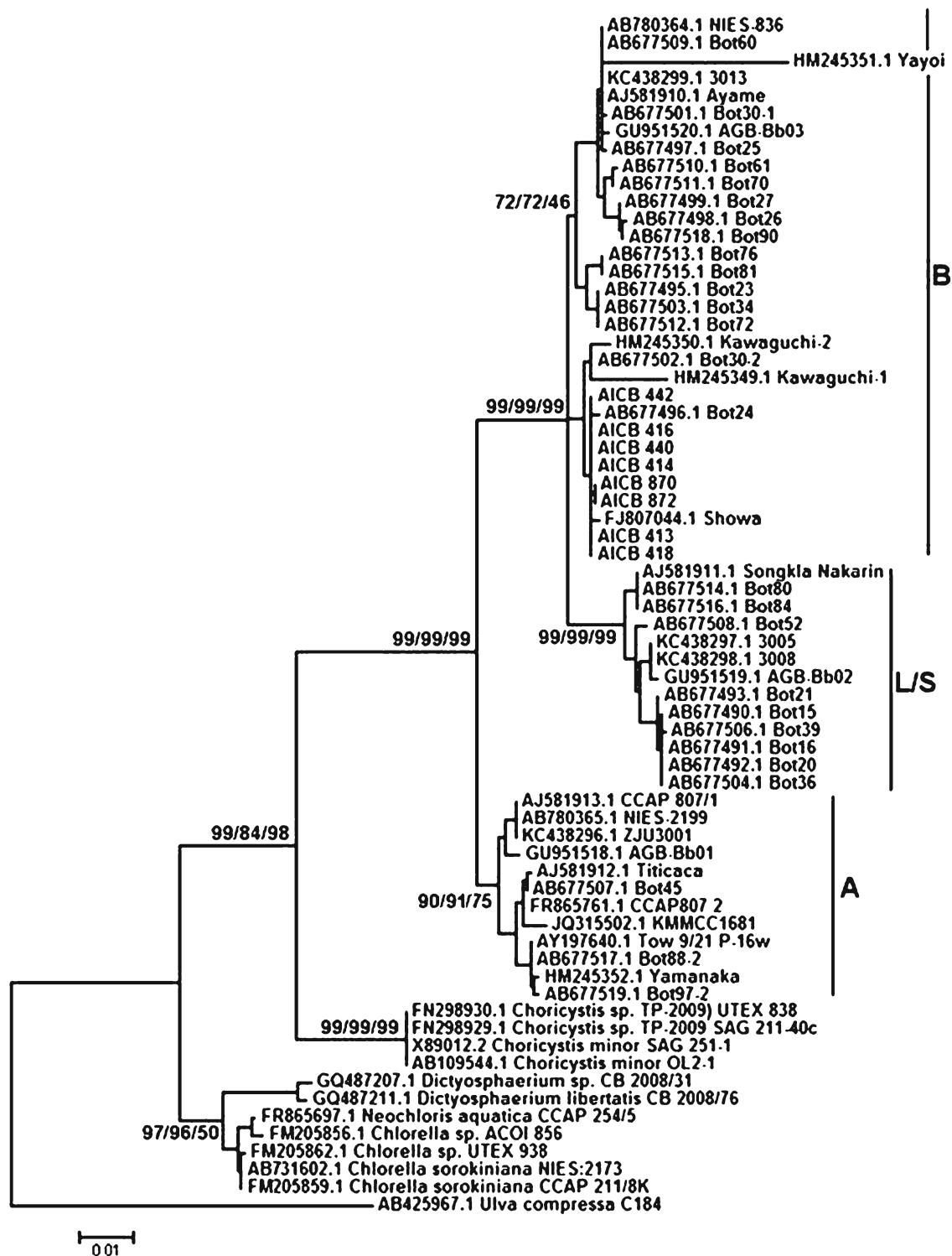
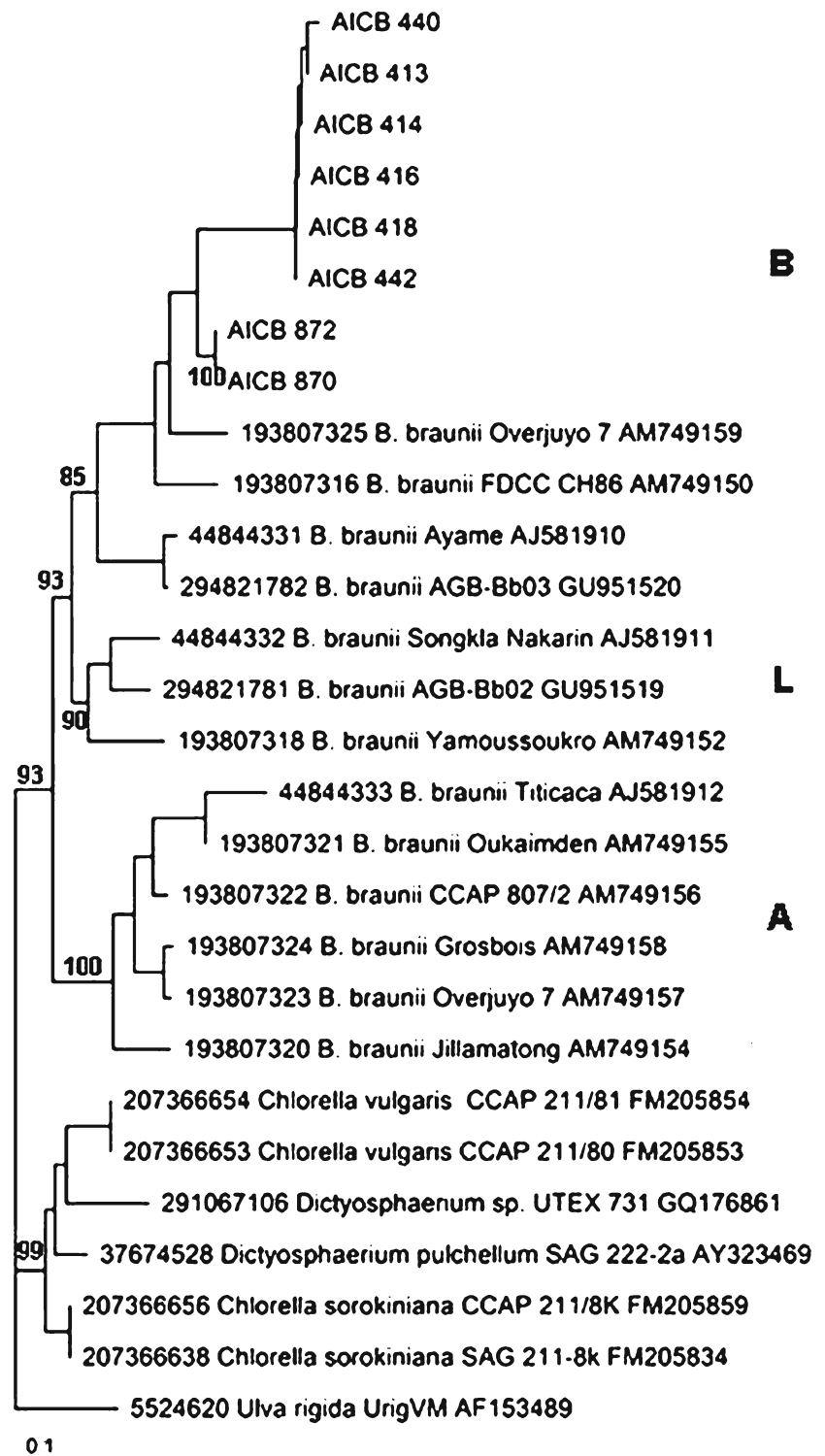


Fig. 4 Phylogenetic tree of the 18S rDNA sequences inferred by the ML method. The main clades are supported by bootstrap values obtained in NJ, MP, and ML methods (1,000, 1,000, and 100 replicates, respectively)

considered as another important diagnostic character of *B. terribilis* species, as the cells of *B. braunii* are “never completely closed” in their cup-shaped mucilaginous sheaths (Komárek and Marvan 1992).

For the first time, ultrastructural details of the *B. terribilis* cell envelope revealed a high degree of similarity with other *Botryococcus* strains (Wolf and Cox 1981; Berkaloff et al. 1984; Weiss et al. 2012). Even if there is a terminology issue

Fig. 5 Phylogenetic tree of the ITS2 sequences-structures inferred by PNJ, using 4SALE and ProfDistS. The main clusters are supported by bootstrap values obtained with MEGA 6.06, using ML method (100 replicates)



in the studies mentioned above (different terms were used for the same ultrastructural feature), we identified similar features in *B. terribilis* AICB strains. Thus, the CW of our strains corresponded to the description of Weiss et al. (2012), and it was entirely covered by a thin lucent layer, named TLS by Wolf and Cox (1981). Although Weiss et al. (2012) did not use

the same terminology, they also identified a thin white tubular layer resembling “toothpaste” at the base of what they described as the “retaining wall” (RW). Furthermore, they mentioned that this structure remained attached to the CW, while the G layer of the RW (which formed fibrils in the apical part of the cell) detached to form the “drapes” and “zipper-like”

formations between adjacent cells. These structures were also identified in our strains, when cells were adjacent (Fig. 3d). In addition, when cells were separated by folds of hydrocarbons, our images were very similar to the descriptions of Wolf and Cox (1981) and Berkaloff et al. (1984), who noticed TLSs alternating with hydrocarbon layers.

The absence of the cap in *B. terribilis* (Komárek and Marvan 1992; de Queiroz Mendes et al. 2012) but its presence in our *B. terribilis* strains certify that some previously made conclusions regarding the variability of this character (Fanés Treviño et al. 2010) may be considered valid. Furthermore, Komárek and Marvan (1992) and Wolf and Cox (1981) pointed out the presence of the mucilaginous cap in strains of *B. braunii*, while Weiss et al. (2012) noticed no such feature in the case of *B. braunii* Showa. We also noticed the presence/absence of the cap in cells from the same colony. Based on our findings, we propose here a possible three-step mechanism to explain the transitory aspect of the cap. (1) In the first stage, each cell possesses the cell wall (CW) and the retaining wall (RW), which forms fibrils in the apical region. In the lateral parts of the cells, the hydrocarbons are externalized (certain amount of membrane and the CW which remains associated with the basal tubular layer (T) of the RW) (Fig. 3g). Thus, the granular layer (G) of the RW is pushed laterally, creating the zipper-like formations between cells (Fig. 3d) (Weiss et al. 2012). (2) When a certain amount of hydrocarbon is externalized, the cell produces a new CW+RW. The new RW will also produce its fibrillar structures in the apical region pushing the old CW+RW toward outside the colony (and thus creating the cap structure) (Fig. 3e). At the same time, new hydrocarbon molecules are released through the plasma membrane and the new CW–T associated layers, pushing the G layer of the new RW laterally. In this way, this new G layer becomes associated with the old CW+T layers, creating a trilaminar structure (TLS), which alternates with hydrocarbon folds (Fig. 3g). This conclusion might be in agreement with both our observations and those of Wolf and Cox (1981) which pointed out the existence of a lucent material often associated on one or both sides with electron dense material. (3) When hydrocarbon droplets accumulate laterally, they create a pressure in the apical region of the old CW+RW layers, creating a rupture in the middle area (pointed out by asterisk in Fig. 3h). The two resulting apical parts fall down on the laterally newly formed hydrocarbon fold covered by the G layer of the new RW. Thus, the content of the cap (which bears fibrils) is now exposed to the growth medium. Such a possible mechanism would explain the presence of regions that exude peripheral fibrils where cells were parted by folds of hydrocarbons (Fig. 3a). In addition, the chemistry of the cap which accumulates “polysaccharide material” (Blackburn and Temperley 1936) seems to be similar to the results of Weiss et al. (2012) who highlighted the arabinose and galactose content of the fibrils.

The appearance of the organelles like mitochondria or the starch and plastoglobules containing chloroplast which showed a basal pyrenoid crossed by chloroplast lamellae together with the presence of lipid bodies resembled the descriptions of both *B. terribilis* FW-15 (de Queiroz Mendes et al. 2012) and *B. braunii* (Wolf and Cox 1981; Berkaloff et al. 1984; Weiss et al. 2012). In addition, the characteristics of the central nucleus, the apical placement of the Golgi body, and the occurrence of ER cisternae associated with the plasma membrane, chloroplast, and nucleus were in agreement with ultrastructural descriptions of *B. braunii* (Weiss et al. 2012).

Growth and chemical profile

The growth rates obtained for *B. terribilis* AICB strains (0.20–0.3) (data not shown) were higher than those obtained for *B. terribilis* IBL C115 (0.14) (Nascimento et al. 2013), but similar to other data regarding *B. braunii* (Ben-Amotz et al. 1985; Li and Qin 2005; Dayananda et al. 2006; Rao et al. 2007; Yeesang and Cheirsilp 2011). Considering studies focused on growth optimization, we assume that the process might be improved for the AICB 440 strain which possessed the highest doubling time (4.62 days). A plausible explanation was offered, though, for the slow growth rate issue of *Botryococcus* strains (Melis 2013), which limits endeavors aiming to improve the growth performance. According to the author’s findings, the Showa strain possesses an inherent diminished photosynthetic carbon flux toward sugars (40–45 %) (compared to 80–85 % in plants and cyanobacteria), leading to slower growth rates, while the rest of the carbon flux is used in terpenoids (45 %) and fatty acid (10 %) synthesis. Thus, due to the metabolic constraints, it would be difficult to obtain strains which produce high amounts of hydrocarbons and have growth rates similar to other chlorophycean microalgae (e.g., a doubling time of 0.28 days in *Neochloris* sp. according to Ben-Amotz et al. (1985)). The ability of *Botryococcus* strains belonging to the B chemical race to synthesize large amounts of terpenoids, as demonstrated in the case of the Showa strain (Melis 2013), is also related to the botryococcene and carotenoid content (both having isoprene origin). The Chl/Car ratios (around 2:1) obtained in the inspected *B. terribilis* AICB strains followed similar profiles as described for the Showa (Eroglu and Melis 2010; Eroglu et al. 2011) and Kawaguchi-1 (Eroglu et al. 2011) B-race strains. Slight differences were noticed in the profiles of AICB 870 and AICB 872, both strains having a larger content of chlorophylls, similar to other green algae (e.g., 2.05 % of DW in *Chlamydomonas reinhardtii* CC503) (Eroglu et al. 2011).

Unfortunately, there is little data regarding *B. terribilis* in the scientific literature (Komárek and Marvan 1992; Fanés Treviño 2009, 2010; Nogueira and Oliveira 2009; Rodrigues et al. 2010; de Queiroz Mendes et al. 2012; Nascimento et al.

2013), and until now, there are no experimental data to ascertain the hydrocarbon profile in other strains of this species. The hydrocarbon mixtures obtained for the AICB strains corresponded to the main features assigned to the B chemical race strains (significant quantities of botryococenes accompanied by small fractions of alkadienes) (Metzger et al. 1985a). A difference was noted though regarding the prevalence of the C₃₀–C₃₂ botryococenes in our hydrocarbon extracts, while the dominant fractions in the Showa strain were the C₃₃ and C₃₄ botryococenes (Wolf et al. 1985). In this matter, some authors suggested a variation in the process of botryococcene methylation (and thus the chain elongation) in relation to the growth conditions (Metzger et al. 1985a; Okada et al. 2004). In addition, the occurrence of C₃₂ as the dominant fraction among the botryococenes was established in other strains belonging to the B chemical race (Okada et al. 1995). As for the amounts of hydrocarbons resulted from our experiments, their values are comparable with those obtained by Okada et al. (1995), who reported values ranging from 9.75 to 37.9 % of dry biomass for some B strains (Kawaguchi-1 and -2, Darwin, Berkeley, and Yayoi). In conclusion, the presence of botryococenes as major fractions in the hydrocarbon extracts attested the affiliation of *B. terribilis* AICB strains to the B chemical race.

Our experiments showed comparable results with other studies which ascertained the presence of the four dominant fatty acids (in the same ascending order) in the *B. terribilis* IBL-C115 strain isolated from Brazil (Nascimento et al. 2013) and in a tropical *Botryococcus* strain (Sahu et al. 2013). Our results were also similar to the outcomes of previous studies, where oleic, palmitic, and linoleic acids (Metzger et al. 1989) or oleic, palmitic, and linolenic acids (Ben-Amotz et al. 1985) accounted for the large majority of fatty acids. The last authors also pointed out the variability of fatty acid amounts in relation to the growth conditions. Since all AICB strains were cultured in similar growth conditions and the biomass was harvested and processed in the same way, we conclude that the inherent variability of the AICB strains is directly responsible for the small variations we obtained in the fatty acid dominant fractions. In fact, this aspect was intensively explored by some researchers (Dayananda et al. 2006), who noticed the influence of culture age, nitrogen source, and pH on the fatty acid relative content in SAG 30.81 and LB 572 *Botryococcus* strains (A chemical race). A beneficial aspect regarding the future use of these strains as potential lipid sources is pointed out by their ability to synthesize polyunsaturated fatty acids (PUFAs—EPA and DHA). These two acids were identified in significant percentages, 20.18 % for EPA (AICB 870) and 11.67 % for DHA (AICB 872) (Table 4), when compared with the best results (7.6 % for EPA) obtained by Ben-Amotz et al. (1985) who studied the LB 572 strain. Even though our results suggested the ability of *B. terribilis* strains to synthesize significant amounts of PUFAs, we could not extend this

conclusion further to other studied strains. This remark is based on two reasons: (i) the only *B. terribilis* strain studied so far from this perspective (IBL-C115) produced neither EPA nor DHA acid (Nascimento et al. 2013), and (ii) variations in the relative amounts of fatty acids are known to occur when growth parameters are modified (Dayananda et al. 2006).

Phylogenetic placement of the AICB strains based on SSU rDNA and ITS2 fragments

Using the 18S rRNA genes, Weiss et al. (2010, 2011) established the phylogenetic relationship between the three chemical races and different strains of *Botryococcus*. Using the same molecular marker, Kawachi et al. (2012) described not only a fourth chemical race (S) but also subclades within the B cluster, suggesting that “the genetic divergence of *Botryococcus* genus is extremely high for it to be assigned to just one species.” It most probably goes beyond the A, B, and L classification, giving credit to the work of Komárek and Marvan (1992), who noticed the variability of this genus based on morphological criteria. Our phylogenetic analysis based on 18S rRNA gene sequences revealed a single subclade formed by the AICB strains in the race B clade, together with Bot24 and Showa strains and a cluster separated from other B-race sequences in the ITS2 sequence-structure tree. Thus, all the AICB strains affiliated to *B. terribilis* based on morphological grounds (the presence of mucilaginous processes and the cells partially or completely embedded in the matrix) formed a convincing clade in both phylogenetic analyses we performed. Even if some authors contested the stability of the morphological characters in designating new species of *Botryococcus* (Plain et al. 1993), our findings lead to the conclusion that the affiliation of the AICB strains to *B. terribilis* based on morphological criteria reflects the phylogenetic reality. Interestingly, the 18S rRNA sequences of two strains assigned to *B. braunii* (Showa and Bot24) were placed in the same cluster with *B. terribilis* AICB strains. This grouping might be due to the high level of phylogenetic heterogeneity of the species *B. braunii* which leads to the conclusion of Kawachi et al. (2012) that *B. braunii* should be split into “at least two species.” Also, by using the ITS2 sequence-structure assay, we intended to strengthen the clustering inferred by the 18S rRNA analysis. Unfortunately, the number of ITS2 sequences available in the public database is too low, and there is a need for more homologous sequences to increase the resolution of the ITS2 phylogeny. The present data suggest that the diversity of the genus *Botryococcus* is still a provoking issue, and in order to widen the view of the phylogenetic relationships among its strains, the 18S rRNA approach have to be supported by additional molecular markers (e.g., ITS1 and ITS2) corroborated by both morphological and biochemical observations.

References

- Allen MM, Stanier RY (1968) Growth and divisions of some unicellular blue-green algae on plates. *J Gen Microbiol* 51:199–202
- Arnon DI (1949) Copper enzymes in isolated chloroplasts. Polyphenyloxidase in *Beta vulgaris*. *Plant Physiol* 24:1–15
- Audino M, Grice K, Alexander R, Kagi RI (2002) Macrocyclic alkanes in crude oil from the algaenan of *Botryococcus braunii*. *Org Geochem* 33:979–984
- Baba M, Shiraima Y (2013) Biosynthesis of lipids and hydrocarbons from algae. In: Dubinsky Z (ed) *Photosynthesis*, 1st edn. InTech, Rijeka, p 336
- Ben-Amotz A, Tomabene TG, Thomas WH (1985) Chemical profile of selected species of microalgae with emphasis on lipids. *J Phycol* 21:72–81
- Benson DA, Karsch-Mizrachi I, Lipman DJ, Ostell J, Wheeler DL (2008) GenBank. *Nucleic Acids Res* 36:D25–D30
- Berkaloff C, Coute A, Casadevall E, Rousseau B, Metzger P, Chirac C (1984) Variability of cell wall structure and hydrocarbon type in different strains of *Botryococcus braunii*. *J Phycol* 20:377–389
- Blackburn KB, Temperley BN (1936): A reinvestigation of the alga *Botryococcus braunii* Kützing In: Robert Grant & Son (ed) *Botryococcus the algal coals*, Transactions of the Royal Society of Edinburgh, Edinburgh
- Bligh EG, Dyer WJ (1959) A rapid method of extraction and purification of total lipids. *Can J Biochem Phys* 37:911–917
- Britton G, Liaaen-Jensen S, Pfänder H (1995) Carotenoids. Volume 1A: isolation and analysis. BirkhäuserVerlag, Basel, Boston, Berlin
- Casadevall E, Metzger P, Puech M-P (1984) Biosynthesis of triterpenoid hydrocarbons in the alga *Botryococcusbraunii*. *Tetrahedron Lett* 25:4123–4126
- Casadevall E, Dif D, Largeau C, Gudin C, Chaumont D, Desanti O (1985) Studies on batch and continuous cultures of *Botryococcus braunii*: hydrocarbon production in relation to physiological state, cell ultrastructure, and phosphate nutrition. *Biotechnol Bioeng* 27:286–295
- Christie WW (1993) *Advances in lipid methodology—two*. Oily Press, Dundee
- Comas GA (1996) Las Chlorococcalesdulciacuícolas de Cuba. *Bibliotheca Phycologica*, 99, J. Cramer, Stuttgart. 192 pp
- Dayananda C, Sarada R, Shamala TR, Ravishankar GA (2006) Influence of nitrogen sources on growth, hydrocarbon and fatty acid production by *Botryococcus braunii*. *Asian J Plant Sci* 5:799–804
- de Queiroz Mendes MC, Comas González AA, Vieira Moreno ML, Pereira Figueira C, de Castro Nunes JM (2012) Morphological and ultrastructure features of a strain of *Botryococcus terribilis* (Trebouxiophyceae) from Brazil. *J Phycol* 48:1099–1106
- Drago N, Péterfi L, Momeu L, Popescu C (1997) An introduction to the algae and the culture collection of algae at the Institute of Biological Research Cluj-Napoca. Cluj University Press, Cluj-Napoca
- Eroglu E, Melis A (2010) Extracellular terpenoid hydrocarbon extraction and quantitation from the green microalgae *Botryococcus braunii* var. Showa *Bioresource Technol* 101:2359–2366
- Eroglu E, Okada S, Melis A (2011) Hydrocarbon productivities in different *Botryococcus* strains: comparative methods in product quantification. *J Appl Phycol* 23:763–775
- Fanés Treviño I, Sánchez-Castillo P, Comas González A (2009) Contribution to the taxonomic study of the family Botryococcaceae (Trebouxiophyceae, Chlorophyta) in southern Spain. *Cryptogamie Algal* 30:17–30
- Fanés Treviño I, Sánchez-Castillo P, Comas González A (2010) Nuevas citas de algas verdes Cocales en la Península Ibérica. *Bol R SocEspHist Nat Sec Biol* 104:5–24
- Friedrich J, Dandekar T, Wolf M, Müller T (2005) ProfDist: a tool for the construction of large phylogenetic trees based on profile distances. *Bioinformatics* 21:2108–2109
- Ghasemi Y, Rasoul-Amini S, Naseri AT, Montazeri-Najafabady N, Mobasher MA, Dabbagh F (2012) Microalgae biofuel potentials (Review). *Appl Biochem Microbiol* 48:126–144
- Goodwin TW (1976) *Chemistry and biochemistry of plant pigments*, 2nd eds. Academic Press, New-York
- Guillard RRL (1973) Division rates. In: Stein JR (ed) *Handbook of Phyycological Methods, Culture Methods and Growth Measurements*. Cambridge University Press, Cambridge, pp 289–312
- Guindon S, Gascuel O (2003) A simple, fast and accurate method to estimate large phylogenies by maximum-likelihood. *Syst Biol* 52:696–704
- Hillen LW, Pollard G, Wake LV, White N (1982) Hydrocracking of the oil of *Botryococcus braunii* to transport fuels. *Biotechnol Bioeng* 24:193–205
- Hindák F (1991) *Botryococcus canadensis*, spec. nova (Chlorophyceae, Chlorococcales). *Arch Protistenkd* 139:55–58
- Kalendar R, Lee D, Schulman AH (2011) Java web tools for PCR, in silico PCR, and oligonucleotide assembly and analysis. *Genomics* 98:137–144
- Kawachi M, Tanoi T, Demura M, Kaya K, Watanabe MM (2012) Relationship between hydrocarbons and molecular phylogeny of *Botryococcus braunii*. *Algal Res* 1:114–119
- Koetschan C, Förster F, Keller A, Schleicher T, Ruderisch B, Schwarz R, Müller T, Wolf M, Schultz J (2010) The ITS2 database III: homology modelling RNA structure for molecular systematics. *Nucleic Acids Res* 38:D275–D279
- Koetschan C, Hackl T, Müller T, Wolf M, Förster F, Schultz J (2012) ITS2 database IV: interactive taxon sampling for internal transcribed spacer 2 based phylogenies. *Mol Phylogenet Evol* 63:585–588
- Komárek J, Marvan P (1992) Morphological differences in natural populations of *Botryococcus* (Chlorophyceae). *Arch Protistenkd* 141:65–100
- Komárková J (1991) Life cycle of *Botryococcus protuberans* W. et G. S. WEST in natural conditions. *Arch Protistenkd* 139:59–68
- Kützing FT (1849) *Species algarum*. FA Brockhaus, Lipsiae [Leipzig]
- Lanave C, Preparata G, Saccone C, Serio G (1984) A new method for calculating evolutionary substitution rates. *J Mol Evol* 20:86–93
- Largeau C, Casadevall E, Berkaloff C (1980a) The biosynthesis of the long-chain hydrocarbon in the green alga *Botryococcus braunii*. *Phytochemistry* 19:1081–1085
- Largeau C, Casadevall E, Berkaloff C, Dharmelincourt P (1980b) Sites of accumulations and composition of hydrocarbons in *Botryococcus braunii*. *Phytochemistry* 19:1043–1051
- Li Y, Qin JG (2005) Comparison of growth and lipid content in three *Botryococcus braunii* strains. *J Appl Phycol* 17:551–556
- Melis A (2013) Carbon partitioning in photosynthesis. *Curr Opin ChemBiol* 17:1–4
- Merget B, Wolf M (2010) A molecular phylogeny of Hypnales (Bryophyta) inferred from ITS2 sequence-structure data. *BMC Res Notes* 3:320
- Metzger P, Casadevall E (1987) Lycopadiene, a tetraterpenoid hydrocarbon from new strains of the green alga *Botryococcus braunii*. *Tetrahedron Lett* 28:3931–3934
- Metzger P, Largeau C (2005) *Botryococcus braunii*: a rich source for hydrocarbons and related ether lipids. *Appl Microbiol Biotechnol* 66:486–496
- Metzger P, Berkaloff C, Casadevall E, Coute A (1985a) Alkadiene- and botriococcene- producing races of wild strains of *Botryococcus braunii*. *Phytochemistry* 24:2305–2312
- Metzger P, Casadevall E, Pouet MJ, Pouet Y (1985b) Structures of some botryococcenes: branched hydrocarbons from the B-race of the green alga *Botryococcus braunii*. *Phytochemistry* 24:2995–3002
- Metzger P, Templier J, Largeau C, Casadevall E (1986) A n-alkatriene and some n-alkadienes from the A race of the green alga *Botryococcus braunii*. *Phytochemistry* 25:1869–1872

- Metzger P, David M, Casadevall E (1987) Biosynthesis of triterpenoid hydrocarbons in the B-race of the green alga *Botryococcus braunii*. Sites of production and nature of the methylating agent. *Phytochemistry* 26:129–134
- Metzger P, Villarreal-Rosales E, Casadevall E, Couté A (1989) Hydrocarbons, aldehydes and triacylglycerols in some strains of the A race of the green alga *Botryococcus braunii*. *Phytochemistry* 28:2349–2353
- Metzger P, Pouet Y, Bischoff R, Casadevall E (1993) An aliphatic polyaldehyde from *Botryococcus braunii* (A race). *Phytochemistry* 32:875–883
- Moldowan JM, Seifert WK (1980) First discovery of botryococenes in petroleum. *J Chem Soc Chem Comm* 19:912–914
- Müller T, Rahmann S, Dandekar T, Wolf M (2004) Accurate and robust phylogeny estimation based on profile distances: a study of the Chlorophyceae (Chlorophyta). *BMC Evol Biol* 4:20
- Nascimento IA, Marques SSI, Cabanelo ITD, Pereira SA, Druzian JI, de Souza CO, Vich DV, Carvalho GC, Nascimento MA (2013) Screening microalga strains from biodiesel production: lipid productivity and estimation of fuel quality based of fatty acids profiles as selective criteria. *Bioenerg Res* 6:1–13
- Nogueira IS, Oliveira JE (2009) Chlorococcales e Ulothricales de hábito colonial de quatrolagosartificiais do município de Goiânia—GO. *Iheringia, Porto Alegre* 64:123–143
- Okada S, Murakami M, Yamaguchi K (1995) Hydrocarbon composition of newly isolated strains of the green microalga *Botryococcus braunii*. *J Appl Phycol* 7:555–559
- Okada S, Devarenne TP, Murakami M, Abe H, Chappell J (2004) Characterization of botryococcene synthase enzyme activity, a squalene synthase-like activity from the green microalga *Botryococcus braunii*, Race B. *Arch Biochem Biophys* 422:110–118
- Olsson S, Buchbender V, Enroth J, Huttunen S, Hedenäs L, Quandt D (2009) Evolution of the Neckeraceae (Bryophyta) resolving the backbone phylogeny. *Syst Biodivers* 7:419–432
- Page R (1996) TreeView: An application to display phylogenetic trees on personal computers. *Comput Appl Biosci* 12:357–358
- Plain N, Largeau C, Derenne S, Couté A (1993) Variabilité morphologique de *Botryococcus braunii* (Chlorococcales, Chlorophyta): corrélations avec les conditions de croissance et la teneur en lipides. *Phycologia* 32:259–265
- Poole CF (2003) *The essence of chromatography*. Elsevier, Amsterdam
- Posada D (2003) jModelTest: Phylogenetic model averaging. *Mol Biol Evol* 25:1253–1256
- Rahmann S, Müller T, Dandekar T, Wolf M (2006) Efficient and robust analysis of large phylogenetic datasets. In: Hsu H-H (ed) *Advanced Data Mining Technologies in Bioinformatics*. Idea Group Inc., Hershey, pp 104–117
- Rao AR, Dayananda C, Sarada R, Shamala TR, Ravishankar GA (2007) Effect of salinity on growth of green alga *Botryococcus braunii* and its constituents. *Bioresour Technol* 98:560–564
- Rodrigues LL, Sant’Anna CL, Tucci A (2010) Chlorophyceae das represas Billings (Braço Taquacetuba) e Guarapiranga, SP, Brasil. *Rev Bras Bot* 33:247–264
- Sahu A, Pancha I, Jain D, Paliwal C, Gosh T, Patidar S, Bhattacharya S, Mishra S (2013) Fatty acids as biomarkers of microalgae. *Phytochemistry* 89:53–58
- Sawayama S, Inoue S, Yokoyama S (1995) Phylogenetic position of *Botryococcus braunii* (Chlorophyceae) based on small subunit ribosomal RNA sequence data. *J Phycol* 31:419–420
- Schultz J, Maisel S, Gerlach D, Müller T, Wolf M (2005) A common core of secondary structure of the internal transcribed spacer 2 (ITS2) throughout Eukaryota. *RNA* 11:361–364
- Schultz J, Müller T, Ahtzinger M, Seibel PN, Dandekar T, Wolf M (2006) The internal transcribed spacer 2 database—a web server for (not only) low level phylogenetic analyses. *Nucleic Acids Res* 34:W704–W707
- Seibel PN, Müller T, Dandekar T, Schultz J (2006) Wolf M (2006) 4SALE—a tool for synchronous RNA sequence and secondary structure alignment and editing. *BMC Bioinformatics* 7:498
- Seibel PN, Müller T, Dandekar T (2008) Wolf M (2008) Synchronous visual analysis and editing of RNA sequence and secondary structure alignments using 4SALE. *BMC Res Notes* 1:91
- Selig C, Wolf M, Müller T, Dandekar T, Schultz J (2008) The ITS2 database II: homology modelling RNA structure for molecular systematics. *Nucleic Acids Res* 36:D377–D380
- Senousy HH, Beakes GW, Hack E (2004) Phylogenetic placement of *Botryococcus braunii* (Trebouxioiophyceae) and *Botryococcus sudeticus* isolate UTEX 2629 (Chlorophyceae). *J Phycol* 40:412–423
- Summons RE, Metzger P, Largeau C, Murray AP, Hope JM (2002) Polymethyl squalenes from *Botryococcus braunii* in lacustrine sediments and crude oils. *Org Geochem* 33:99–109
- Sutherland IW, Wilkinson JF (1971) Chemical extraction methods from microbial cells. In: De Warris JR, Ribbons DW (eds) *Methods of Microbiology* volume 5B. Acad Press, London, pp 350–356
- Tamura K, Nei M (1993) Estimation of the number of nucleotide substitutions in the control region of mitochondrial DNA in humans and chimpanzees. *Mol Biol Evol* 10:512–526
- Tamura K, Stecher G, Peterson D, Filipski A, Kumar S (2013) MEGA6. Molecular evolutionary genetics analysis version 6.0. *Mol Biol Evol* 30:2725–2729
- Wake LV, Hillen LW (1980) Study of “bloom” of the oil-rich alga *Botryococcus braunii* in the Darwin river reservoir. *Biotechnol Bioeng* 22:1637–1656
- Wake LV, Hillen LW (1981) Nature and hydrocarbon content of blooms of the alga *Botryococcus braunii* occurring in Australian freshwater lakes. *Aust J Mar Freshwat Res* 32:353–367
- Watanabe MM, Tanabe Y (2013) Biology and industrial potential of *Botryococcus braunii*. In: Richmond A, Hu Q (eds) *Handbook of Microalgal Culture*, vol 2nd. Wiley-Blackwell, Oxford, pp 369–387
- Watanabe MM, Kawachi M, Hiroki M, Kasai F (2000) NIES-Collection List of Strains. Microalgae and Protozoa. Microbial Culture Collections, 6th edn. National Institute for Environmental Studies, Tsukuba, p 159
- Weiss TL, Johnston JS, Fujisawa K, Sumimoto K, Okada S, Chappell J, Devarenne TP (2010) Phylogenetic placement, genome size, and GC content of the liquid-hydrocarbon-producing green microalga *Botryococcus braunii* strain Berkeley (Showa) (Chlorophyta). *J Phycol* 46:534–540
- Weiss TL, Johnston JS, Fujisawa K, Okada S, Devarenne TP (2011) Genome size and phylogenetic analysis of the A and L races of *Botryococcus braunii*. *J Appl Phycol* 23:833–839
- Weiss TL, Roth R, Goodson C, Vitha S, Black I, Azadi P, Rusch J, Holzenburg A, Devarenne TP, Goodenough U (2012) Colony organization in the green alga *Botryococcus braunii* (race B) is specified by a complex extracellular matrix. *Eukaryot Cell* 11:1424–1440
- Wolf FR, Cox ER (1981) Ultrastructure of active and resting colonies of *Botryococcus braunii* (Chlorophyceae). *J Phycol* 17:395–405
- Wolf FR, Nonomura AM, Basshan JA (1985) Growth and branched hydrocarbon production in a strain of *Botryococcus braunii* (Chlorophyta). *J Phycol* 21:388–396
- Wolf M, Ruderisch B, Dandekar T, Müller T (2008) ProfdistS: (profile-) distance based phylogeny on sequence-structure alignments. *Bioinformatics* 24:2401–2402
- Yeesang C, Cheirsilp B (2011) Effect of nitrogen, salt, and iron content in the growth medium and light intensity on lipid production by microalgae isolated from freshwaters sources in Thailand. *Bioresour Technol* 102:3034–3040